Characterization of barium strontium titanate (BST) single crystal nanorods prepared by wet chemical method

R. SENGODAN, B. CHANDAR SHEKAR[a,*]
Department of Physics, Kumaraguru College of Technology, Coimbatore- 641049 Tamil Nadu, India
[a]Departments of Physics, Kongunadu Arts and Science College, G.N- Mills, Coimbatore- 641029, Tamil Nadu, India

Barium strontium titanate nanoparticles were synthesized by the wet chemical method using the starting materials as barium chloride ($BaCl_2$), titanium dioxide (TiO_2), strontium carbonate ($SrCO_3$) and oxalic acid sintered at 900 C. The composition of the particle was identified by EDS. The crystalline structure investigated by X-ray diffraction show that the nanoparticles exhibit a tetragonal BST phase. Rod like morphology was observed by scanning electron microscope (SEM). TEM images revealed that the BST nanoparticles are rod like morphology with diameter of about 50 – 100 nm. FTIR measurement showed the existence of Ba-Sr-Ti-O bond in the nanoparticles. Optical properties were studied by using UV-Visible spectrophotometer. The band gap of the particles was found to be 2.73 eV. It was found to be direct allowed transition. The absorption co-efficient (α) and extinction co-efficient (K) were also evaluated ad reported in this paper.

(Received December 3, 2013; accepted July 10, 2014)

Keywords: Barium strontium titanate, XRD, TEM, SEM, FTIR, UV – Visible

1. Introduction

A number of titanate-based ferroelectric materials have been investigated in the past for tunable device applications. These ferroelectrics are used as phase shifters, resonators, filters and capacitors in communication systems [1]. The solid solution of Barium Strontium Titanate (BST) has emerged as a strong candidate material for such applications. $Ba_xSr_{1-x}TiO_3$ is a continuous solid solution between $BaTiO_3$ and $SrTiO_3$ over its entire composition range [2]. Dielectric permittivity of BST is dependent on composition and temperature and, can be tuned on application of a DC electric field [3]. BST exhibits a maximum dielectric permittivity in the temperature range 0–390 K [4] and possesses attractive properties required for tunable applications [5].

The dielectric constant and intrinsic losses of ferroelectric materials depend on their process of synthesis, microstructure and, dopants used [6]. Various processes like sputtering, laser ablation, chemical vapor deposition (CVD), solid-state processing and wet chemical have been used to synthesize BST powder and its thin films for ferroelectric applications. However, there is still a need to evolve better process and technology to synthesize reliable tunable material, with reduced dielectric constant and material loss tangent; while possessing higher tunability so as to get optimum K factor (tunability/loss tangent). Some of these existing challenges and needs might find solution in the arena of nano-technology and nano-materials, which exhibit some of the extraordinary properties due to their unusual chemical and/or synergistic properties. In order to make ferroelectric materials compatible to semiconductor processing techniques nano range thin films is a necessity. High frequency thin film BST device design is generally based on two approaches. The first uses thin films of thickness <50 nm and the second approach uses thicker films generally >300 nm. Thin films of BST doped with magnesium have been synthesized with an average grain size of 25 nm, low dielectric loss of 0.007 and dielectric constant of 386 [7]. Wet chemical synthesis of tunable, non-linear dielectric materials offer advantages like low temperature synthesis, ease in controlling the composition variations, low cost and potential use in film processing. It is believed that nano-sized materials can offer modified electron sensitive properties [8] and better sinterability [9]. Earlier studies on synthesis of crystalline BST powder resulted in powder of 0.8–2.7 μm [10] using a solid-state reaction route. Selvam and Kumar [11] reported the synthesis of 50 nm BST powder by direct precipitation method. Shen et al. [12] successfully synthesized 100 nm BST powder using nitrate based precursor solutions. Addition of ethyl alcohol during the process further reduced the powder grain size.

Widespread application of BST for use as parallel plate capacitor in tunable microwave devices demand good sintering characteristic at low temperatures of around 900° C. This would also enable the use of BST in low temperature co-fired ceramic (LTCC) structures [13]. Nanocrystalline powder, because of their high diffusivity, can be sintered at lower temperatures compared to their polycrystalline coarse grain counterparts [14]. Consequently, in order to meet the two requirements of thin film applicability and low sintering temperatures, there is a need for nanocrystalline BST powder with improved properties. Nanoscale BST powder can also be used to fabricate ferroelectric particle dispersed

nanocomposites exhibiting intelligent functions like predicting and controlling of crack initiation and growth [15].

The objective of this research was to synthesize single crystal nanoroads BST powder below 70 nm via a simple wet chemical process, which could be easily reproduced and to study its sintering behavior.

2. Experimental details

2.1 Synthesis of $BaSrTiO_3$ nanoparticles

$BaSrTiO_3$ nanoparticles were synthesized using Wet chemical method. The starting materials used were barium chloride ($BaCl_2.2H_2O$), stanium dioxide (TiO_2), strontium carbonate ($SrCO_3$) and oxalic acid. A solution of Ba: Ti: oxalic acid: $SrCO_3$ having mole ratio1: 1: 1: 0.1 was stirred and evaporated at 70°C till a clear, viscous resin was obtained and then dried at 110° C for 20 hours. The precursor formed was heated at 900° C for 2 hours to form $BaSrTiO_3$ nanoparticles

Sample preparation

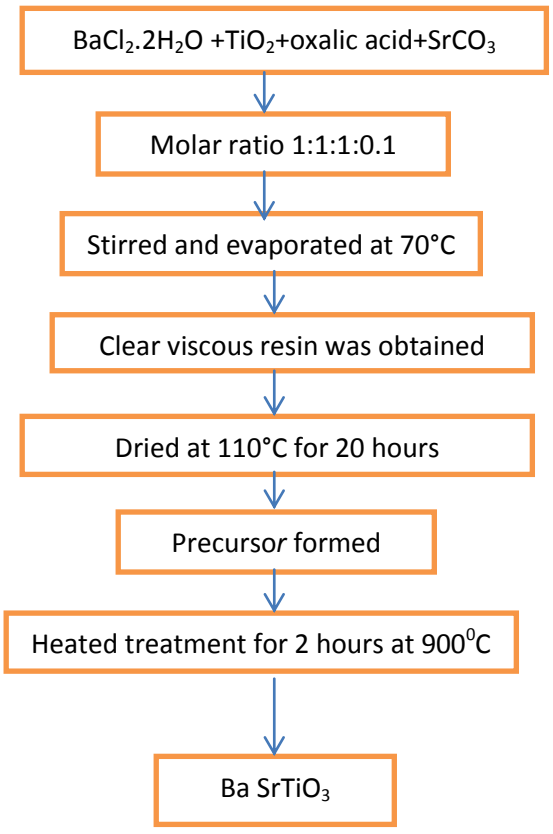

2.2 Characteristics of $BaSrTiO_3$ nanoparticles

FTIR and Energy Dispersive X-ray micro analyser (EDS) were used for the identification of the chemical composition. The XRD patterns of the resulting products were obtained from X- ray powder diffraction with CuKα radiation. The micrograph of $BaSrTiO_3$ was examined by direct observation via scanning electron microscope (SEM). The high-resolution transmission electron microscopy (HRTEM) images were obtained with a JEOL-2010 microscopy at an acceleration voltage of 200kV. The optical reflectance measurements were made by using JASCO-UV/VISIBLE spectrophotometer (model UVIDEC 610, Japan).

3. Result and discussion

3.1 EDS analysis

Energy dispersive spectrum (EDS) analysis was carried out to identify the composition of the $BaSrTiO_3$ nanoparticles. Fig. 1 shows the EDS of the $BaSrTiO_3$ nanoparticles. EDS analysis indicates the presence of Ba, Sr, Ti and O in the synthesized nanoparticles. High intensity peaks corresponding to Ba and Ti elements were clearly noticed in the EDS patterns.

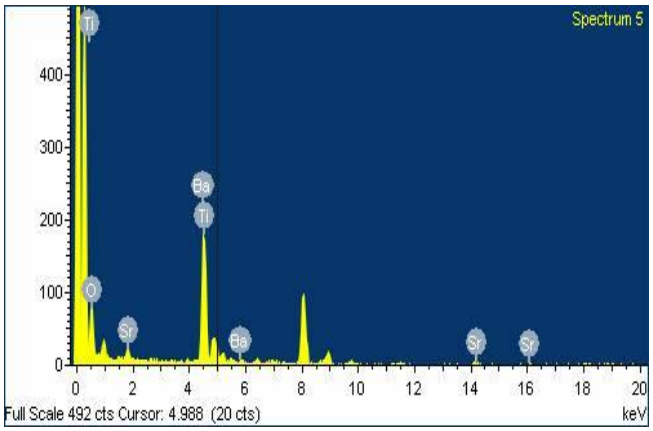

Fig. 1. EDS spectrum of of $BaSrTiO_3$ nanoparticle.

3.2 FTIR analysis

The formation of $BaSrTiO_3$ was further evaluated by FTIR measurements as shown in Fig. 2. The FTIR studies of $BaSrTiO_3$ shows the small absorption bands at around 3452.96, 1629.27, 1433.83, 1008.85, 669.9 and 566.65 cm^{-1}. The band centred at 3424.25 cm^{-1} corresponds to lattice water absorbed (antisymmetric and symmetric OH stretching) [16]. The band at 1629.27 cm^{-1} is due to the organic groups bonded to titanium. The 1433.83 cm^{-1} band is due to CH_2 – CO bending vibrations or – COOH bands which are coupled by O-H bending vibrations and C – O stretching vibrations. The 1008.85 cm^{-1} band is probably due to characteristic band where metal ions combined with acetic radical (M – CH_3COO) [17]. The bands at 699.69 and 566.65 cm^{-1} are mainly due to the formation of metal oxides (M – O: Ba – O, Sr – O, Ti – O).

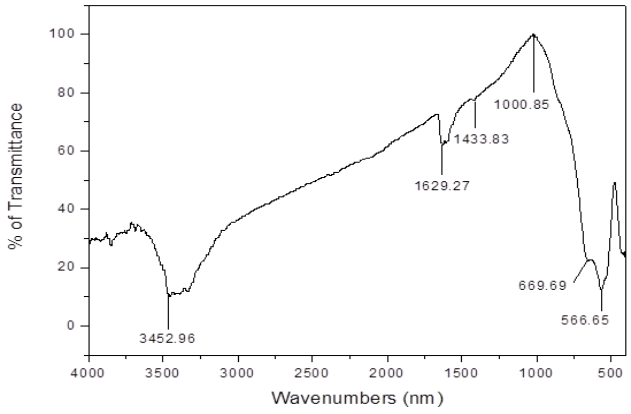

Fig. 2. FTIR spectrum of $BaSrTiO_3$ nanoparticles.

3.3 X – ray diffraction analysis

Fig. 3 shows the XRD pattern of $BaSrTiO_3$ nanoparticles. From XRD measurement, of the $BaSrTiO_3$ particle exhibited tetragonal structure, because the peak splitting was found clearly in the (002) plane, which shows its high degree of tetragonality [18, 19].

The grain size is calculated from the Scherrer's formula from the full with half – maximum (FWHM) of the XRD peaks

$$D=0.94\lambda/\beta\cos\theta \quad (1)$$

The crystalline size (D) was calculated at high intensity peak (100) plane was 66 nm.

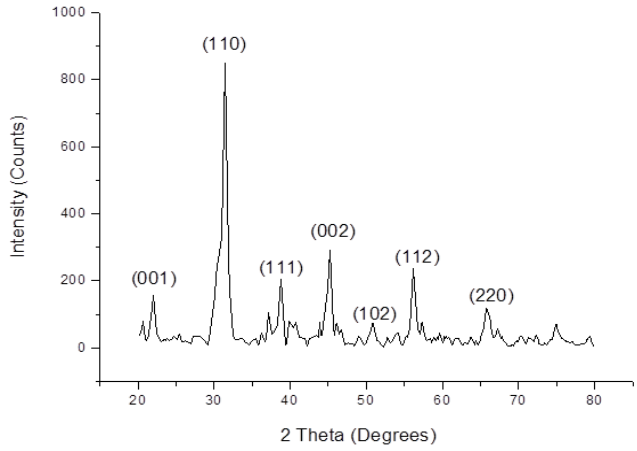

Fig. 3. XRD spectrum of $BaSrTiO_3$ nanoparticles.

3.4 SEM analysis

Fig. 4 shows the SEM images of $BaSrTiO_3$ particles. Rod like shape of nanoparticles distributed throughout the particles. The irregular shape suggested diffusion of barium source in the TiO_2 particle [20].

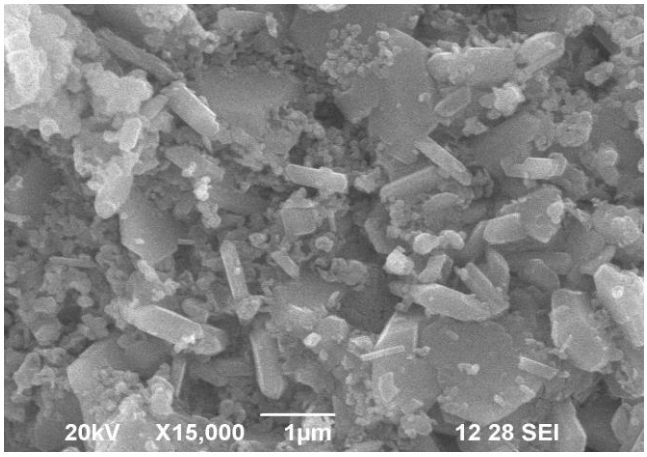

Fig. 4. SEM Micrograph of $BaSrTiO_3$ nanoparticles.

3.5 TEM images

Fig. 5a shows the HRTEM micrography of the $BaSrTiO_3$ nanoparticles with a well -isolated rod like morphology. The diameter of the rod is about 50 – 70 nm. Fig. 5b is the SAED pattern of the $BaSrTiO_3$ nanorods, which reveals that the nanoparticles exhibit a tetragonal single structure. Fig. 5c shows the fringing spacing of the nanorod. According to the image, well- resolved lattice fringes can be seen clearly, which give further information on fine micro-structure of the rod like $BaSrTiO_3$ nanoparticles. The fringe spacing of 2.857 A˚ corresponds to the (110) planes of nanoparticles. This is also confirmed by XRD analysis.

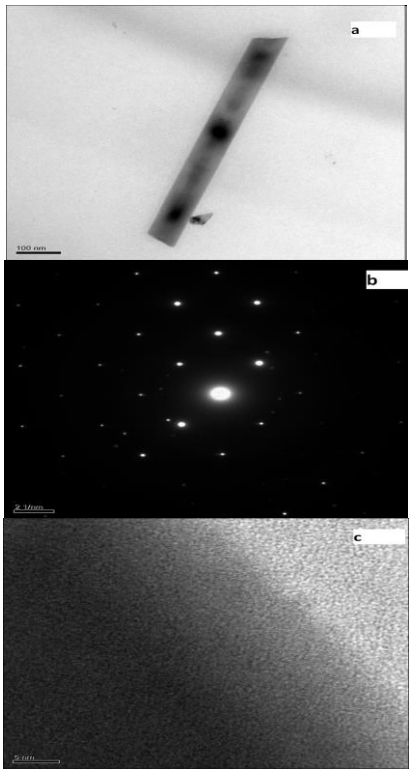

Fig. 5. TEM images of $BaSrTiO_3$ nanoparticles
(a) nanorod (b) SAED pattern (c) the fringing spacing.

3.6 Optical properties

Fig. 6 shows the reflectance spectra of the $BaSrTiO_3$ nanoparticles. It reveals that the reflectance increases with the increase of the wavelength up to 900 nm and then decreases with increase of wavelength, which may be due to more absorption in the infrared region.

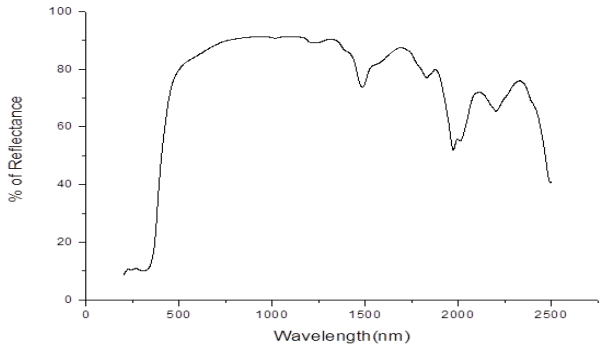

Fig. 6. Reflectance spectrum of $BaSrTiO_3$ nanoparticles.

From the reflected spectra the extinction co-efficient (k) can be calculated from the relation,

$$k = 2.303\lambda \log (1/T_0)/4\pi d \quad (2)$$

Where d is the size of the particles and λ wavelength of the light. The absorption co-efficient (α) can be calculated from

$$\alpha = 4\pi k/\lambda \quad (3)$$

Fig. 7 represents the variation of extinction coefficient (k_f) with wavelength of $BaSrTiO_3$ nanoparticles. It is observed that the extinction coefficient increases with increase of wavelength. It has been observed that in general the extinction coefficient increases with increase in photon energy.

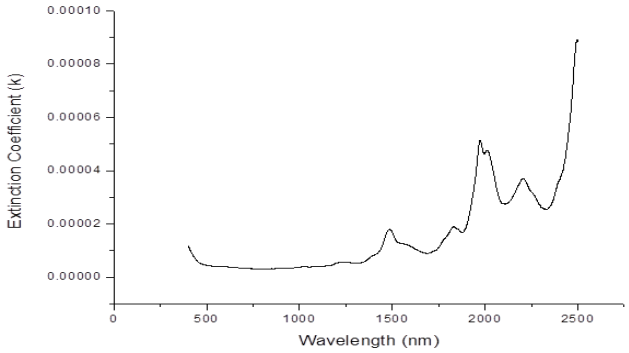

Fig. 7. Variation of Extinction co-efficient (k) with wavelength for $BaSrTiO_3$nanoparticles.

Fig. 8 shows the variation of absorption coefficient with wavelength of $BaSrTiO_3$ nanoparticles. It is observed that a steep fall in absorption coefficient up to nearly the wavelength of 800 nm and there after it increases with the increase of the wavelength.

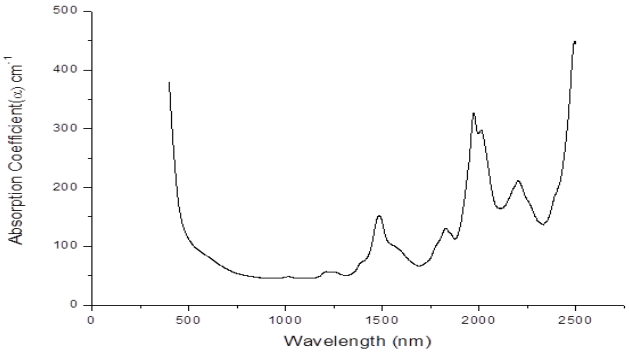

Fig. 8. Variation of absorption co-efficient (α) with wavelength for $BaSrTiO_3$ nanoparticles.

For direct allowed transition the absorption coefficient and photon energy are related by expression.

$$\alpha h\nu = A\,(h\nu - E_g)^n \quad (4)$$

Where A is a constant and E_g the optical band gap energy. The variation of $(\alpha h\nu)^2$ versus photon energy (hν) of $BaSrTiO_3$ particles is shown in Fig. 9. Extrapolation of the linear portion of the curve to $(\alpha h\nu)^2 = 0$ gives the optical band gap value for the nanoparticles. The plot show straight line portion supporting the interpretation of direct and allowed band gap for the nanoparticles. The energy gap of the nanoparticles was found to be 2.73 eV. It is good agreement with the earlier investigations on $BaSrTiO_3$ nanoparticles (21).

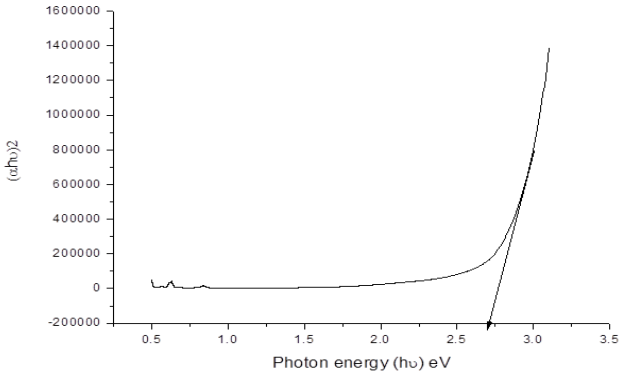

Fig. 9. Variation of $(\alpha h\nu)^2$ versus photon energy (hν) of $BaSrTiO_3$ nanoparticles.

4. Conclusion

We have successfully synthesized $BaSrTiO_3$ nanoparticles by low cost wet chemical method using commercially available chemicals such as oxalic acid, TiO_2, $BaCl_2$ and $SrCO_3$. The composition of $BaSrTiO_3$ nanoparticles were confirmed by EDS and FTIR analysis. XRD indicated that the particles have tetragonal structure. The rods like morphology were found in SEM and TEM micrographs. The absorption co-efficient and extinction coefficient of the particles were determined from optical reflection spectra. Optical band gap of $BaSrTiO_3$ particles was found to be direct allowed.

References

[1] Vikas Somani, Samar Jyoti Kalita, J Electroceram **18**, 57 (2007).

[2] P. C. Joshi, M. W. Cole, Appl. Phys. Lett, **77**(2), 289 (2000).

[3] I. P. Koutsaroff, T. Bernacki, M. Zelner, A. Cervin-Lawry, A. Kassam, P. Woo, L. Woodward, A. Patel, Mater. Res. Soc. Symp. Proc. **784**, 319 (2004).

[4] A. K. Tagantsev, V. O. Sherman, K. F. Astafiev, J. Venkatesh, N. Setter, J. Electroceramics **11**, 5 (2003).

[5] K.T. Kim, C.-I. Kim, Thin Solid Films **472**, 26–30 (2004).

[6] M. Jain, S. B. Majumder, R. S. Katiyar, A. S. Bhalla, Thin Solid Films **447–448**, 537 (2004).

[7] M. W. Cole, P. C. Joshi, M. H. Ervin, M. C. Wood, R. L. Pfeffer, Thin Solid Films **374**, 34 (2000).

[8] H. Gleiter, J. Weissmuller, O. Wollersheim, R. Wurschum, Acta Mater. **49**, 737 (2001).

[9] J. F. Chen, Z. G. Shen, F. T. Liu, X. L. Liu, J. Yun, Scr. Mater. **49**, 509 (2003).

[10] B. Su, J. E. Holmes, B. L. Cheng, T. W. Button, J. Electroceramics **9**, 111 (2002).

[11] I. Packia Selvam, V. Kumar, Mater. Lett. **56**, 1089 (2002).

[12] C. Shen, Q. F. Liu, Q. Liu, Mater. Lett. **58**, 2302 (2004).

[13] T. Hu, H. Jantunen, A. Uusimaki, S. Leppavuori, Mater. Sci. Semicond. Process. **5**, 215 (2003).

[14] C. Suryanarayana, C. C. Koch, Hyperfine Interact. **130**, 5 (2000)

[15] H. J. Hwang, T. Nagai, M. Sando, M. Toriyama, K. Niihara, J. Eur. Ceram. Soc. **19**, 993 (1999).

[16] Jaspreet kaur, Kotnala R. K, Kuldeep Chand Verma J. Optoelectron. Adv. Mater. **14**, 219 (2012).

[17] Hu Young Tian, Wei Gen Luo, Xing Hua Pu, Ping Sun Qiu, Xi Yun He, Ai Li Ding Thermochimica Acta **360**, 57 (2000).

[18] D. Begg, Bruce, Vance, R. Eric, Nowotny, Janusz, J Am Ceram Society **77**, 3186 (1994).

[19] B. D. Stojannovic, A. Z. Simoes, C. O. Paiva – santos, j Eur Ceram Soc **25**, 1985 1989 (2005).

[20] U. Manzoor, D. K. Kim, J. Mater Sci Technol **23**, 655 (2007).

[21] Valeria Morases Longo, Maria das Graca Sampaio Costa, Alexandre Zirpole Simoes, Ieda Lucia Viana Rosa, Carlos Oliveria Paiva Santos, Juan Andres, Elson Longo, Jose Arana Varela Phys Chem Chem Phys **12**, 7566 (2010).

*Corresponding author: chandar.bellan@gmail.com